





## Research Article

# Low-Molecular-Weight Hydrolysate from Black Goat Extract Had Antioxidative and Anti-Inflammatory Effects in Macrophage Cells via Inhibition of MAPKs and NF- $\kappa$ B Pathways

Hye-Jin Kim <sup>1,2</sup>, Kwan-Woo Kim <sup>3</sup>, Jinwook Lee <sup>4</sup>, Sang-Hoon Lee <sup>5</sup>,  
Sung-Soo Lee <sup>3</sup> and Aera Jang <sup>1</sup>

<sup>1</sup>Department of Applied Animal Science, College of Animal Life Science, Kangwon National University, Chuncheon 24341, Republic of Korea

<sup>2</sup>Center for Food and Bioconvergence, Seoul National University, Seoul 08826, Republic of Korea

<sup>3</sup>Animal Genetic Resources Research Center, National Institute of Animal Science, Rural Development Administration, Hamyang 50000, Republic of Korea

<sup>4</sup>R & D Coordination Division, National Institute of Animal Science, Rural Development Administration, Jeonju 54875, Republic of Korea

<sup>5</sup>Grassland and Forages Division, National Institute of Animal Science, Rural Development Administration, Cheonan 31000, Republic of Korea

Correspondence should be addressed to Aera Jang; [ajang@kangwon.ac.kr](mailto:ajang@kangwon.ac.kr)

Received 2 May 2023; Revised 25 December 2023; Accepted 29 December 2023; Published 8 January 2024

Academic Editor: Rafik Balti

Copyright © 2024 Hye-Jin Kim et al. This is an open access article distributed under the Creative Commons Attribution License, which permits unrestricted use, distribution, and reproduction in any medium, provided the original work is properly cited.

This study evaluated the antioxidative and anti-inflammatory effects of a low-molecular-weight hydrolysate derived from black goat extract using alcalase, ProteAX, and trypsin (APT6 < 3 kDa). The APT6 < 3 kDa exhibited high antioxidative activities with estimated contents of 41.24% for antioxidative amino acids and 49.55% for hydrophobic amino acids. APT6 < 3 kDa inhibited nitric oxide and prostaglandin  $E_2$  production in RAW 264.7 cells induced by lipopolysaccharide ( $p < 0.05$ ), which was accompanied by the inhibition of inducible nitric oxide synthase and cyclooxygenase-2 protein expression. Additionally, APT6 < 3 kDa downregulated the mRNA expression and production of TNF- $\alpha$  and IL-1 $\beta$  ( $p < 0.05$ ). Mechanistically, these anti-inflammatory effects of APT6 < 3 kDa were shown by downregulating the MAPK and NF- $\kappa$ B pathways in a dose-dependent manner. Overall, 43 peptides were isolated from a certain fraction (F5) of APT6 < 3 kDa, demonstrating high antioxidative and anti-inflammatory activities. These results suggest that identified peptides from APT6 < 3 kDa possess natural antioxidants and hold potential as anti-inflammatory agents.

## 1. Introduction

Excessive calorie intake and exposure to stress and pollution can generate harmful radicals in the body, including reactive oxygen species (ROS). Various circumstances such as oxidative stress, tissue damage, pathogen invasion, or exposure to lipopolysaccharides (LPS) resembling endotoxins, activate the immune system, encompassing both innate and adaptive immunity. This immune response involves diverse types of immune cells including macrophages, natural killer

cells, neutrophils, and T and B lymphocytes. Macrophages play a protective role against oxidative stress by secreting prostaglandin  $E_2$  (PGE $_2$ ), nitric oxide (NO), and proinflammatory cytokines through the expression of inflammatory proteins [1]. The activation of these intracellular signaling pathways initiates inflammatory processes [2]. While inflammation is recognized as a major defense mechanism in the body, excessive macrophage activation from inflammation can contribute to the development of serious diseases such as diabetes, cancer, atherosclerosis, and

arthritis [3]. As this is highly related to oxidative stress, antioxidative agents play a protective role in inflammatory conditions [4].

Synthetic antioxidants such as butylated hydroxytoluene and butylated hydroxyanisole are commonly employed to inhibit oxidative reactions and inflammation [3]. However, their usage is constrained by potential side effects. Natural sources, foods, and ingredients encompass a wide array of functional compounds that have antioxidative properties, thereby contributing to the maintenance of human health [5]. Bioactive peptides typically exist in inactive forms within parent proteins, and their active forms are released through enzymatic hydrolysis [6].

Several proteolytic enzymes including trypsin, alcalase, ProteAX, flavourzyme, FoodPro® alkaline protease, pancreatin, and protease P have been employed to generate antioxidative hydrolysates and peptides from diverse sources. These sources encompass a variety of origins, including fish, milk, marine species, soybean, and plant [7, 8], donkey skin [9], and pig skin [10]. Especially, the bioactive peptides with low molecular weight are acknowledged for their potent antioxidative activity and several other functionalities, which are attributed to their ability to easily traverse the intestinal barrier [11]. Previous studies have reported the diverse functionalities of low-molecular-weight peptides (<3 kDa) on cells [9, 10, 12].

Black goat meat is recognized as a nutritious animal protein due to its low-fat content and abundance of essential amino acids and minerals, such as Ca and Fe [13]. In Korea, not only the meat but also the meat and bones of the black goat are consumed in the form of an extract that is prepared by processing the entire black goat carcass with Korean medicinal herbs under high temperature and pressure. This extract is well known to enhance the immune system and anti-inflammatory function in young children, pregnant women, and the elderly [13].

The aim of the current study was to assess the antioxidative and anti-inflammatory effects of low-molecular-weight hydrolysate (<3 kDa) derived from black goat extract (termed "APT6 <3 kDa") on macrophage cells and to investigate the underlying mechanism of action. Furthermore, peptides exhibiting substantial antioxidative and anti-inflammatory activities were isolated and identified from APT6 <3 kDa.

## 2. Materials and Methods

**2.1. Chemicals and Reagents.** Alcalase 2.4L (2.4 AU/g, alkaline protease), ProteAX (1,400 U/g, proteases), and trypsin (1,000–2,000 BAEE units/mg, protease from the porcine pancreas) were purchased from Novozymes (Novo Nordisk, Bagsvaerd, Denmark), Amano Enzyme (Nagoya, Aichi, Japan), and Sigma-Aldrich (St. Louis, MO, USA), respectively. An ultrafiltration membrane with a 3 kDa molecular weight cutoff was obtained from Millipore (Bedford, MA, USA). RAW 264.7 macrophages were purchased from the American Type Culture Collection (ATCC TIB-71; Manassas, VA, USA). Dulbecco's modified Eagle's medium (DMEM) was obtained from Welgene (Daegu, Korea).

Penicillin-streptomycin (P/S) stock solution was purchased from Biowest (Nuaille, France). Heat-inactivated fetal bovine serum (FBS) was purchased from Tissue Culture Biologicals (Seal Beach, CA, USA). 3-(4,5-Dimethyl-2-thiazolyl)-2,5-diphenyltetrazolium bromide (MTT), dichlorofluorescein-diacetate (CM-H<sub>2</sub>DCFDA), Escherichia coli 055: B5 LPS, and dimethyl sulfoxide (DMSO) were obtained from Sigma-Aldrich. Griess reagent (Cat# G2930) for the nitric oxide assay was purchased from Promega (Madison, WA, USA). Enzyme-linked immunosorbent assay (ELISA) kits for the quantification of interleukin (IL)-1 $\beta$  (Cat# DY008) and PGE<sub>2</sub> (Cat# KGE004B) were obtained from R & D Systems (Minneapolis, MN, USA), and kits to quantify IL-6 (Cat# 555240) and tumor necrosis factor (TNF)- $\alpha$  (Cat# 558534) were obtained from BD Biosciences (San Jose, CA, USA). Radioimmunoprecipitation assay (RIPA) lysis buffer was purchased from ATTO Co. (Tokyo, Japan) and nuclear and cytoplasmic protein extraction kit (Cat# AKR-171) was obtained from Cell Biolabs (San Diego, CA, USA). Primary antibodies against inducible nitric oxide synthase (iNOS), cyclooxygenase-2 (COX-2), nuclear factor kappa-light-chain-enhancer of activated B cells (NF- $\kappa$ B) p65,  $\beta$ -actin, and secondary antibodies were obtained from Santa Cruz Biotechnology (Santa Cruz, CA, USA). Primary antibodies against phospho-extracellular signal-regulated kinase (ERK) 1/2, ERK1/2, c-Jun N-terminal kinase (JNK), phospho-SAPK/JNK, p38, phospho-p38, I $\kappa$ B $\alpha$ , phospho-I $\kappa$ B $\alpha$ , and secondary antibodies were obtained from Cell Signaling Technology (Danvers, MA, USA). All experiments were conducted using an analytical-grade chemical reagent.

**2.2. Preparation of Low-Molecular-Weight Hydrolysate from Black Goat Extract (BGE).** To create a low-molecular-weight hydrolysate from black goat extract (BGE), we followed the procedure outlined in Figure S1. We obtained five female black goats (*Capra hircus coreanae*) with a carcass weight of 10–11 kg and aged 6–9 months from a local meat market in Chuncheon, Korea. The entire black goat carcass (about 60% fresh meat percent) was sliced into small pieces measuring 5  $\times$  5  $\times$  5 cm<sup>3</sup> and washed under running water. Next, we extracted 2.5 kg of meat and bone with 7.5 L of distilled water in an autoclave at 121°C for 10 hours with a slight modification of Kim et al. [14]. Following extraction, we removed the bone and lyophilized the remaining meat and broth, which we subsequently used for hydrolysis. We hydrolyzed the raw material mixture using 0.67% (w/w) of alcalase (pH 8.0, 50°C), ProteAX (pH 7.0, 50°C), and trypsin (pH 8.0, 37°C) enzymes for 2 h (6 h total). The enzymes in the hydrolysate were denatured at 95°C for 10 minutes, resulting in a hydrolysate referred to as "APT6." We separated APT6 under the molecular weight of 3 kDa using an ultrafiltration membrane, which we called ATP6 <3 kDa.

**2.3. Amino Acid Composition Analysis of Hydrolysates.** To determine the amino acid composition of APT6 and APT6 <3 kDa, we utilized an amino acid analyzer (SYKAM S433; Sykam GmbH, Eresing, Germany) [14]. First, we

hydrolyzed the samples with 6 N hydrochloric acid (HCl) at 110°C for 24 h. For the analysis of cysteine and methionine, we treated the samples with performic acid before adding 6 N HCl. Next, we diluted the hydrolyzed samples using 0.2 N sodium citrate buffer (pH 2.2). We equipped the cation exchange column (LCA K06/Na, 4.6 mm × 150 mm, Sykam GmbH, Eresing, Germany) with detection at 570 nm and solvent to flow at a rate of 0.45 mL/min.

#### 2.4. Antioxidative Activities of BGE and the Hydrolysates

**2.4.1. Ferric Reducing Antioxidant Power (FRAP) Activity Assay.** The FRAP assay was conducted as described by Kim et al. [15]. To prepare the FRAP reagent, we mixed acetate buffer, FeCl<sub>3</sub>·6 H<sub>2</sub>O, and 2,4,6-tripyridyl-s-triazine at a ratio of 10:1:1 (v/v/v). We dissolved the samples in distilled water and added 25 μL of dissolved samples or standard (trolox) to 175 μL of the FRAP reagent. The mixture was incubated at 37°C for 30 min in the dark. After incubation, the absorbance was measured at 590 nm (SpectraMax M2e, Molecular Devices, Sunnyvale, CA, USA). The result was expressed as μmol trolox equivalent (TE)/g dry matter.

**2.4.2. 2,2-Azino-bis(3-Ethyl-Benzothiazoline-6-Sulfonic Acid) (ABTS) Radical Scavenging Activity Assay.** The ABTS radical scavenging activity was determined following the method described by Kim et al. [13]. We adjusted the absorbance of the ABTS<sup>+</sup> radical solution to 0.700 ± 0.02 at 735 nm and 30°C, using distilled water. Next, we mixed 50 μL of dissolved samples or standard (trolox) with 950 μL of the ABTS + radical solution and incubated the mixture at 30°C for 30 minutes in the dark. After incubation, we measured the absorbance of the final reaction solution at 735 nm and expressed as μmol TE/g dry matter.

**2.4.3. Oxygen Radical Absorption Capacity (ORAC) Assay.** The ORAC assay was performed using the method outlined by Kim et al. [13]. Briefly, 25 μL of the samples and standard (trolox) dissolved in 75 mM phosphate-buffered saline (PBS, pH 7.4) were added to 150 μL of fluorescein (80 nM) and incubated at 37°C for 15 min. Subsequently, 25 μL of 2,2'-azobis (2-amidinopropane) hydrochloride (150 mM) was added. The changes in absorbance were measured every minute at 37°C at 480 nm (excitation) and 520 nm (emission) and expressed as μmol TE/g of dry matter.

**2.5. Cell Culture and Cell Viability Assay.** Cell culture was carried out for RAW 264.7 cells in DMEM containing 10% FBS and 1% P/S at 37°C in a 5% CO<sub>2</sub> incubator. To assess the cytotoxicity of APT6 < 3 kDa, a 48-well plate was seeded with 5 × 10<sup>4</sup> cells/well and incubated for 24 h. Subsequently, APT6 < 3 kDa was added to the cells (10 to 500 μg/mL) for 1 h prior to the addition of LPS (1 μg/mL) [2, 3, 6, 9, 10]. After the incubation for 24 h, 50 μL of MTT solution (final concentration of 50 μg/mL) was added to each well, and the plate was further incubated at 37°C for 4 h. The MTT formazan crystals were dissolved using DMSO and detected at 540 nm.

**2.6. Nitric Oxide (NO) Production Assay.** The Griess assay was used to measure the NO levels, as described by Kim et al. [2]. RAW 264.7 cells were seeded in a 24-well plate (4 × 10<sup>5</sup> cells/well) and incubated for 24 h. APT6 < 3 kDa was treated at concentrations of 10–500 μg/mL for 1 h before adding LPS (at a concentration of 1 μg/mL) and incubating for another 24 h at 37°C in a 5% CO<sub>2</sub> incubator. The medium was collected and mixed with Griess reagents I and II in a 1:1 ratio (50 μL each) and incubated at 23°C for 20 min. The absorbance was measured at 540 nm.

**2.7. ROS Production Assay.** The method for estimating ROS production was based on CM-H<sub>2</sub>DCFDA dye fluorescence and described by Kim et al. [2]. RAW 264.7 cells were seeded onto 96-well plates (2 × 10<sup>4</sup> cells/well) and cultured. The cells were treated with APT6 < 3 kDa (10 to 500 μg/mL) for 1 h before adding LPS (1 μg/mL) and incubated for 24 h at 37°C in a 5% CO<sub>2</sub> incubator. After removing the medium, CM-H<sub>2</sub>DCFDA (50 μM) was added, and the plate was incubated for 30 min in the dark. The fluorescence was measured using excitation (485 nm) and emission (535 nm) wavelengths.

**2.8. Determination of PGE<sub>2</sub> and Proinflammatory Cytokine Levels.** Commercial ELISA kits were utilized to measure the levels of PGE<sub>2</sub>, TNF-α, IL-6, and IL-1β, following the manufacturers' instructions [2]. RAW 264.7 cells (4 × 10<sup>5</sup> cells/well) were seeded in 24-well plates. The cells were treated with APT6 < 3 kDa at concentrations of 10–500 μg/mL for 1 h, followed by treatment with LPS (1 μg/mL) for 24 h. The PGE<sub>2</sub>, TNF-α, IL-1β, and IL-6 levels in medium were measured.

**2.9. RNA Extraction and Quantitative Reverse-Transcription Polymerase Chain Reaction (RT-qPCR).** mRNA levels of iNOS, COX-2, TNF-α, IL-1β, and IL-6 in RAW 264.7 cells were assessed using RT-qPCR. To conduct the assay, RAW 264.7 cells were treated with APT6 < 3 kDa for 1 hour prior to activation with LPS for 6 h [16]. Total RNA was extracted from the cells, and cDNA was synthesized using a commercially available kit (Qiagen, Hilden, Germany). The ratio of 260:280 nm in all samples was matched in the range of 1.8–2.0. The RT-qPCR reaction was performed using targeted primers (Table S1) and SYBR Green master mix (BioFact, Daejeon, Korea), and the relative mRNA expression was calculated using the 2<sup>-ΔΔC<sub>t</sub></sup> method and normalized to the mRNA expression of the housekeeping gene (β-actin) using a LightCycler 96 instrument (Roche Diagnostics, Penzberg, Germany).

**2.10. Preparation of Cell Lysates for Western Blot Analysis.** RAW 264.7 cells were treated with different concentrations (10–500 μg/mL) of APT6 < 3 kDa for 1 h, followed by stimulation with LPS (1 μg/mL) for 1 h (for NF-κB, IκBα, p-IκBα, and MAPKs) or 24 h (for iNOS and COX-2) at 37°C in a 5% CO<sub>2</sub> incubator, as described in Kim et al. [2]. The cells were then washed twice with chilled PBS, and the total protein was lysed using RIPA lysis buffer with 1X

phosphatase and protease inhibitors. For the analysis of protein expression of the NF- $\kappa$ B pathway, cytoplasmic and nuclear fractions were extracted as per the instructions provided with the commercial protein extraction kit (Cat# AKR-171). Cell lysates were kept at  $-80^{\circ}\text{C}$  before use.

The protein expression levels were analyzed following the protocol outlined by Kim et al. [8]. The proteins in the cell lysate were separated using 10% sodium dodecyl sulfate-polyacrylamide gel electrophoresis. The gel was then transferred onto polyvinylidene difluoride membranes using the semidry method (ATTO). The membranes were blocked for 2 h using 5% skim milk (COX-2, I $\kappa$ B $\alpha$ , p-I $\kappa$ B $\alpha$ , MAPKs,  $\beta$ -actin) and 5% bovine serum albumin (iNOS and NF- $\kappa$ B) in tris-buffered saline with 0.05% Tween-20 (TBST). The primary antibodies against iNOS (1:200), COX-2 (1:200), I $\kappa$ B $\alpha$  (1:1,000), phospho-I $\kappa$ B $\alpha$  (1:1,000), NF- $\kappa$ B (1:200), SAPK/JNK (1:1,000), phospho-SAPK/JNK (1:2,000), ERK1/2 (1:2,000), phospho-ERK1/2 (1:2,000), p38 (1:2,000), and  $\beta$ -actin (1:200) were added to the membranes and incubated at  $4^{\circ}\text{C}$  for 16 h. The membranes were then washed three times and treated with a secondary antibody at  $23^{\circ}\text{C}$  for 2 h. The protein was developed using enhanced chemiluminescence (Cyanagen, Bologna, Italy) and quantified using the Fusion Solo 6S Edge (Vilber-Lourmat, Marne la Vallée, France).

**2.11. Separation and Identification of Peptides Having Anti-oxidative and Anti-Inflammatory Activities in APT6 < 3 kDa.** The protocol for separating and identifying peptides having high antioxidative and anti-inflammatory activities in APT6 < 3 kDa involved several steps (Figure S1). First, lyophilized APT6 < 3 kDa was dissolved in distilled water and separated using chromatography (NGC Quest 10 Plus; Bio-Rad, CA, USA) equipped with a Superdex peptide column (GE Healthcare, Piscataway, NJ, USA). Five fractions (F1, F2, F3, F4, and F5) were obtained at 215 nm. These five fractions were then lyophilized and evaluated for anti-inflammatory activity using the ORAC assay and tested for their ability to inhibit NO and PGE<sub>2</sub> levels in LPS-stimulated RAW 264.7 cells at 250  $\mu\text{g}/\text{mL}$ .

The amino acid sequences of the peptides with the highest antioxidative and anti-inflammatory activities were analyzed by a Triple TOF 5600 system (ABSciex, Foster City, CA, USA) with a YMC-Pack C8 column [11]. A linear gradient method with a flow rate of 0.25 mL/min was employed, where mobile phases A and B consisted of 0.1% formic acid in water and acetonitrile, respectively. The mass spectra were obtained through electrospray ionization in positive mode. The full-scan mass spectra ranged from 360 to 1,800 m/z, and the data was analyzed using Analyst TF 1.7 software and ProteinPilot 4.5.

**2.12. Statistical Analysis.** The experiments were conducted in triplicate, and the statistical analysis was carried out using SAS software v.9.4 (SAS Institute Inc., Cary, NC, USA). The data analysis in the study involved performing a one-way analysis of variance followed by Tukey tests to compare significant differences among the means at the level of

$p < 0.05$ . The results were presented as means and standard errors of the mean (SEM).

### 3. Results and Discussion

**3.1. Amino Acid Composition of APT6 and APT6 < 3 kDa.** The amino acid composition of APT6 and its low-molecular-weight peptide (APT6 < 3 kDa) is shown in Table S2. Glutamic acid and glycine were identified as the two major amino acids in both APT6 and APT6 < 3 kDa, with concentrations ranging from 12.57 to 13.23 g/100 g and 9.94 to 11.18 g/100 g, respectively. This finding is consistent with previous studies that have reported glutamic acid and glycine as the predominant amino acids in other BGEs [14, 17]. Aspartic acid, proline, alanine, leucine, lysine, and arginine were also abundant in APT6 and APT6 < 3 kDa. Following ultrafiltration with a 3 kDa cutoff, threonine, leucine, tyrosine, and phenylalanine were increased, whereas aspartic acid, glycine, and cysteine were decreased. The essential amino acid (EAA) content of APT6 and APT6 < 3 kDa was found to be 32.96% and 35%, respectively, which surpassed the EAA content of black goat meat extract (23.9%) [17] and veal meat and bone hydrolysate (21.82%) [18]. However, the reported EAA content of chicken meat hydrolysate (44.5%) [19] exceeds that of APT6 and APT6 < 3 kDa.

Animal sources hold great potential as raw materials for generating protein hydrolysates that possess high antioxidative properties [20]. The contents of antioxidative amino acids (AAA) and hydrophobic amino acids (HAA) in APT6 and APT6 < 3 kDa were determined to be 42.55% and 50.39%, and 41.24% and 49.55%, respectively (Table S2). The AAA and HAA composition of hydrolysates varies depending on the protein sources and enzymes used. Veal meat and bone hydrolysate produced using nutrase and trypsin had 43.7% AAA and 36.01% HAA [18]. AAA (51.7%) and HAA (43.5%) contents of oyster hydrolysate generated with alcalase were higher and lower, respectively, than those of APT6 and APT6 < 3 kDa [21]. Rapeseed protein hydrolysate produced with alcalase consisted of 37.35% AAA and 38.65% HAA [22], which were lower than the contents in APT6 and APT6 < 3 kDa.

**3.2. Antioxidative Activities of BGE and Its Hydrolysates.** The antioxidative activities (FRAP, ABTS, and ORAC) of BGE and hydrolysates are presented in Table 1. The FRAP, ABTS, and ORAC activities of BGE were measured to be 5, 64.28, and 45.08  $\mu\text{mol TE}/\text{g}$  dry matter, respectively. However, all the antioxidative activities of the hydrolysate (APT6) were found to be significantly higher than those of BGE ( $p < 0.05$ ). Low-molecular-weight hydrolysate (APT6 < 3 kDa) exhibited the highest FRAP, ABTS, and ORAC activities (6.64, 206.98, and 247.44  $\mu\text{mol TE}/\text{g}$  dry matter, respectively). In comparison, the ABTS activity of donkey-hide gelatin hydrolysate (<3 kDa) hydrolyzed with protease P and blue mussel hydrolysate (<1 kDa) prepared with pepsin was reported to be 51.59  $\mu\text{mol TE}/\text{g}$  dry matter [9] and 55.25  $\mu\text{mol TE}/\text{g}$  dry matter [3], respectively, which were substantially lower than the ABTS activity of

TABLE 1: Antioxidative activities of BGE and its hydrolysates.

Treatment	Antioxidative activities ( $\mu\text{mol TE/g dry matter}$ )		
	FRAP	ABTS	ORAC
BGE	5.00 <sup>c</sup>	64.28 <sup>c</sup>	45.08 <sup>c</sup>
Hydrolysate (APT6)	5.52 <sup>b</sup>	150.94 <sup>b</sup>	211.38 <sup>b</sup>
Low-molecular-weight hydrolysate (APT6 < 3 kDa)	6.64 <sup>a</sup>	206.98 <sup>a</sup>	247.44 <sup>a</sup>
SEM	0.043	0.536	2.949

FRAP, ferric reducing antioxidant power activity; ABTS, 2,2-azino-bis(3-ethyl-benzothiazoline-6-sulfonic acid) radical scavenging activity; ORAC, oxygen radical absorption capacity; BGE, black goat extract; APT6, hydrolysate from BGE prepared using alcalase, ProteAX, and trypsin for 2 h each; APT6 < 3 kDa, the low-molecular-weight fraction (<3 kDa) of APT6 hydrolysate; SEM, standard error of the mean. <sup>a-c</sup>Different superscript letters within a column indicate a significant difference at  $p < 0.05$ .

APT6 < 3 kDa. Additionally, APT6 < 3 kDa exhibited higher ORAC activity than hydrolysates from pig skin (141.39  $\mu\text{mol TE/g dry matter}$ ) [23] and catfish protein (16  $\mu\text{mol TE/g}$ ) [20], but lower activity than hydrolysate from donkey hide gelatin (307.26  $\mu\text{mol TE/g dry matter}$ ) [9]. Generally, enzymatic hydrolysis enhances the antioxidative activities compared to those of the original material [9, 23, 24]. It has been reported that antioxidative peptides isolated from various food sources typically range in size from 500 to 1,800 Da. Low-molecular-weight peptides demonstrate greater biological effects due to their ease of intestinal wall penetration [12]. Several studies have highlighted the anti-inflammatory effect of protein hydrolysates exhibiting antioxidative activities [3, 24]. Collectively, our findings suggest that APT6 and APT6 < 3 kDa could serve as natural antioxidants and potentially possess anti-inflammatory properties.

**3.3. Effects of APT6 < 3 kDa on RAW 264.7 Cell Viability.** The effects of APT6 < 3 kDa on RAW 264.7 cell viability are shown in Figure 1. APT6 < 3 kDa at 10–500  $\mu\text{g/mL}$  increased RAW 264.7 cell viability (Figure 1(a)). Following stimulation with LPS for 24 h, the cell viability decreased to 67.94% compared to the control ( $p < 0.05$ ). LPS decreases the viability of RAW 264.7 cells by releasing inflammatory substances acting as cytotoxic agents [25]. The stimulation in this study appeared to induce a lower cell state in RAW264.7 cells, which could affect the impact of agents on the result. However, treatment with 500  $\mu\text{g/mL}$  of APT6 < 3 kDa significantly elevated the cell viability to 86.03% (Figure 1(b)).

In this study, APT6 < 3 kDa at concentrations ranging from 10 to 500  $\mu\text{g/mL}$  did not exhibit any cytotoxic effects on RAW 264.7 cells, and treatment with 500  $\mu\text{g/mL}$  of APT6 < 3 kDa effectively restored the reduced cell viability induced by LPS. Therefore, the concentration range of 10–500  $\mu\text{g/mL}$  was selected to evaluate the anti-inflammatory activity of APT6 < 3 kDa in this study.

**3.4. Effect of APT6 < 3 kDa on NO, PGE<sub>2</sub>, and ROS Production.** In the inflammatory condition, LPS stimulation leads to the upregulation of iNOS and COX-2 expression, resulting in the excessive production of PGE<sub>2</sub> and NO in macrophages [6]. NO is a free radical produced by iNOS, while PGE<sub>2</sub> is

a product of arachidonic acid metabolism by COX-2 [26]. Consequently, NO and PGE<sub>2</sub> serve as representative indicators of an inflammatory response. Consistent with expectations, treatment of RAW 264.7 cells with LPS at a concentration of 1  $\mu\text{g/mL}$  for 24 hours increased the production of NO and PGE<sub>2</sub> production (Figures 1(c) and 1(d)). However, treatment with 100  $\mu\text{g/mL}$  of APT6 < 3 kDa significantly reduced the level of NO from 37.24  $\mu\text{M}$  (LPS only; 100%) to 34.33  $\mu\text{M}$  (92.18%) ( $p < 0.05$ ), and the maximum reduction to 33.27  $\mu\text{M}$  (89.87%) was achieved with 500  $\mu\text{g/mL}$  of APT6 < 3 kDa (Figure 1(c)). Moreover, the production of PGE<sub>2</sub> induced by LPS (100%) was reduced to 91.68% and 70.14% following treatment with 250  $\mu\text{g/mL}$  and 500  $\mu\text{g/mL}$  APT6 < 3 kDa, respectively ( $p < 0.05$ ; Figure 1(d)). These results demonstrated that APT6 < 3 kDa at concentrations of 250 and 500  $\mu\text{g/mL}$  can effectively downregulate the production of NO as well as PGE<sub>2</sub> production in LPS-stimulated RAW 264.7 cells.

Oxidative stress plays a critical role in the development of chronic inflammation and the induction of cellular damage. ROS is generated under imbalanced oxidant conditions in the body [24]. In this study, LPS stimulation resulted in oxidative stress, as evidenced by an increase in ROS production (141.88%) in RAW 264.7 cells. However, treatment with 250  $\mu\text{g/mL}$  of APT6 < 3 kDa significantly suppressed ROS production to 133.13% (Figure 1(e)). This indicates that the antioxidative properties of APT6 < 3 kDa effectively mitigated oxidative stress in LPS-stimulated RAW 264.7 cells. Therefore, the consumption of these dietary antioxidants may confer protection against oxidative stress and prevent the progression of inflammation.

**3.5. Effects of APT6 < 3 kDa on iNOS and COX-2 mRNA and Protein Expression.** To explain the mechanisms underlying the inhibition of NO and PGE<sub>2</sub> levels in RAW 264.7 cells by APT6 < 3 kDa, the mRNA and protein expression levels of iNOS and COX-2 were evaluated. As shown in Figures 2(a) and 2(b), the mRNA levels of iNOS and COX-2 increased following stimulation with LPS (1  $\mu\text{g/mL}$ ) for 6 h compared to RAW 264.7 cells without APT6 < 3 kDa and LPS ( $p < 0.05$ ). However, treatment with APT6 < 3 kDa at concentrations of 100–500  $\mu\text{g/mL}$  significantly inhibited the expression of iNOS, reducing it from LPS-only treatment (100%) to 81.33%–66.77% (Figure 2(a)). Conversely, APT6 < 3 kDa did not exert a significant inhibitory effect on

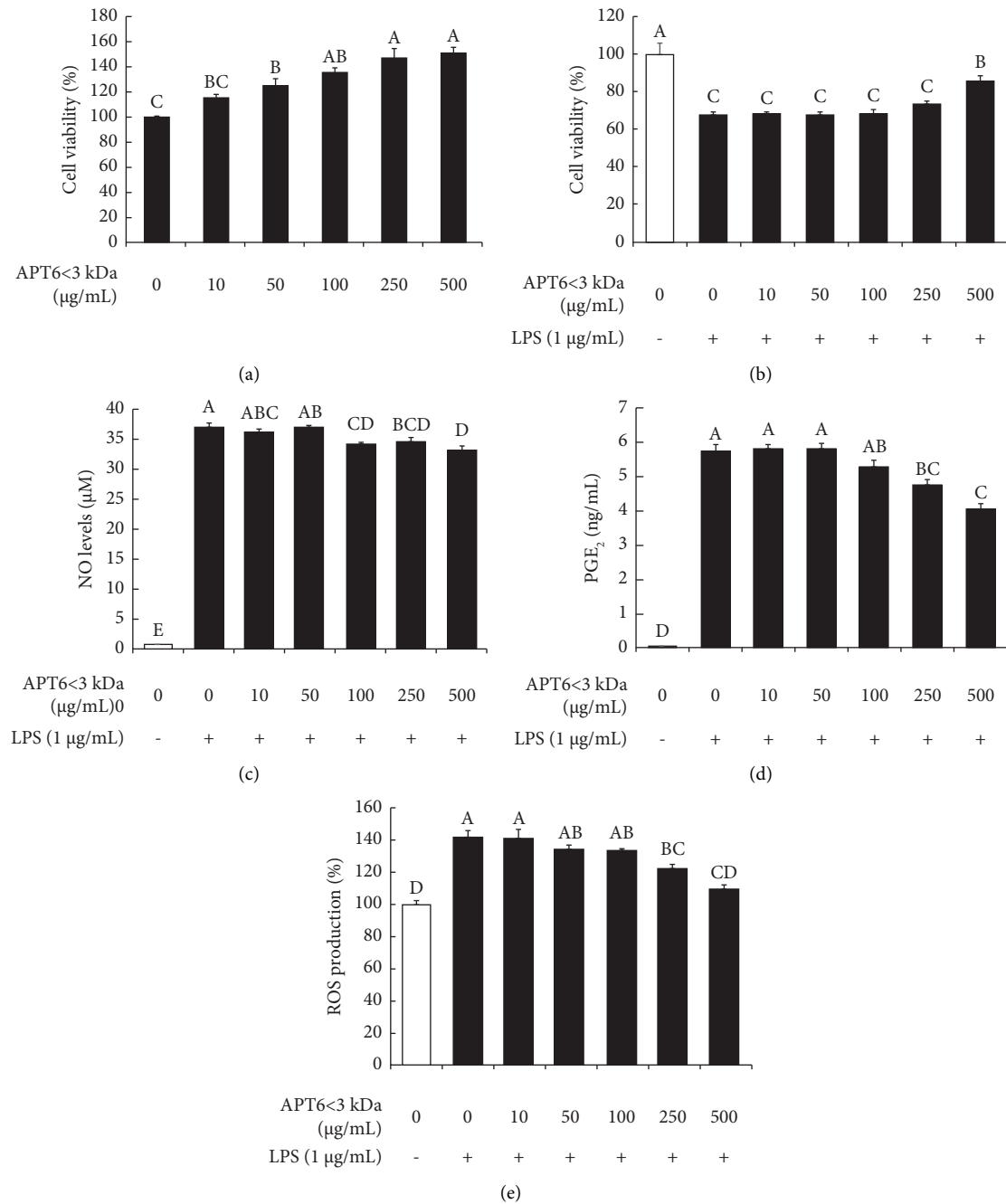


FIGURE 1: Effect of APT6 < 3 kDa on the viability of RAW 264.7 cells without (a) or with stimulation with LPS (1 μg/mL, 24 h; (b)), nitric oxide (NO, (c)), prostaglandin E<sub>2</sub> (PGE<sub>2</sub>, (d)), and reactive oxygen species (ROS, (e)) production after stimulation with LPS (1 μg/mL) for 24 h. APT6 < 3 kDa is the low-molecular-weight fraction (<3 kDa) of BGE hydrolysate prepared by treatment with Alcalase, ProteAX, and trypsin for 2 h each. <sup>A-E</sup>Different superscript letters above bars indicate a significant difference at  $p < 0.05$ .

the expression of COX-2 induced by LPS (Figure 2(b)). The protein expression levels of iNOS and COX-2 were inhibited by APT6 < 3 kDa treatment at concentrations of 50–500 μg/mL compared to the levels observed with LPS-only treatment (Figures 2(c)–2(e);  $p < 0.05$ ). Especially, the protein levels of iNOS decreased to 67.41%, 40.41%, 31.53%, and 26.96% when cells were treated with APT6 < 3 kDa at 50, 100, 250, and 500 μg/mL, respectively, in comparison with the level induced by LPS (100%; Figure 2(d);  $p < 0.05$ ). These

results suggest that the inhibition of NO and PGE<sub>2</sub> production by APT6 < 3 kDa can be attributed to the down-regulation of iNOS and COX-2 expression in LPS-stimulated RAW 264.7 cells.

**3.6. Effects of APT6 < 3 kDa on mRNA Expression and Levels of Proinflammatory Cytokines.** The effect of APT6 < 3 kDa on mRNA expression and production of IL-6, IL-1β, and TNF-

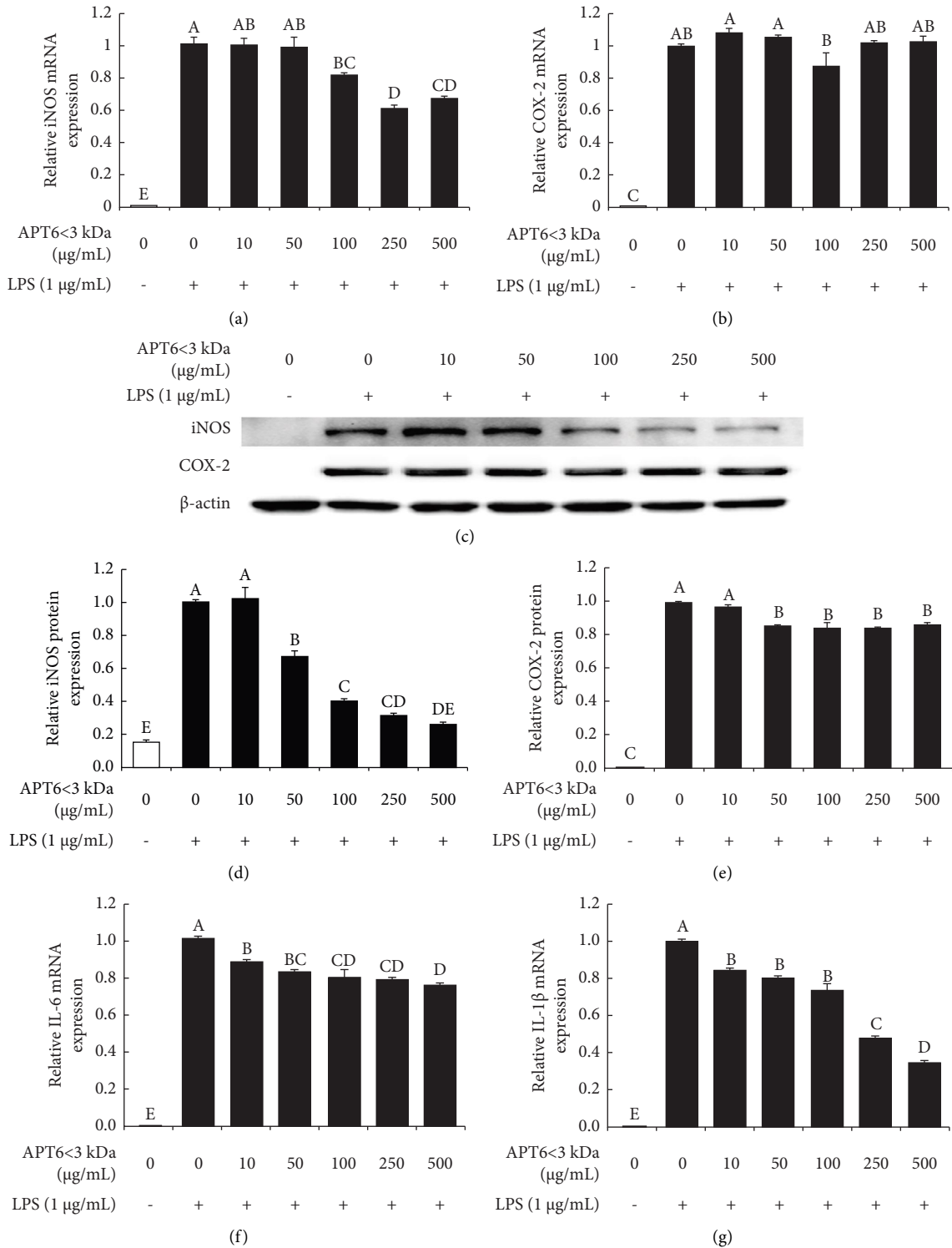


FIGURE 2: Effects of APT6 < 3 kDa on mRNA and protein expression of inducible nitric oxide synthase (iNOS) and cyclooxygenase-2 (COX-2) in LPS-stimulated RAW 264.7 cells. Cells were treated with APT6 < 3 kDa for 1 h and incubated with LPS (1 μg/mL) for 6 h. mRNA levels of iNOS (a), COX-2 (b) were determined by RT-qPCR. To quantify the protein expression of iNOS and COX-2 (c-e), cells were treated with APT6 < 3 kDa for 1 h and incubated with LPS (1 μg/mL) for 24 h. APT6 < 3 kDa is the low-molecular-weight fraction (<3 kDa) of BGE hydrolysate prepared by treatment with Alcalase, ProteAX, and trypsin for 2 h each. <sup>A-E</sup>Different superscript letters above bars indicate a significant difference at *p* < 0.05.

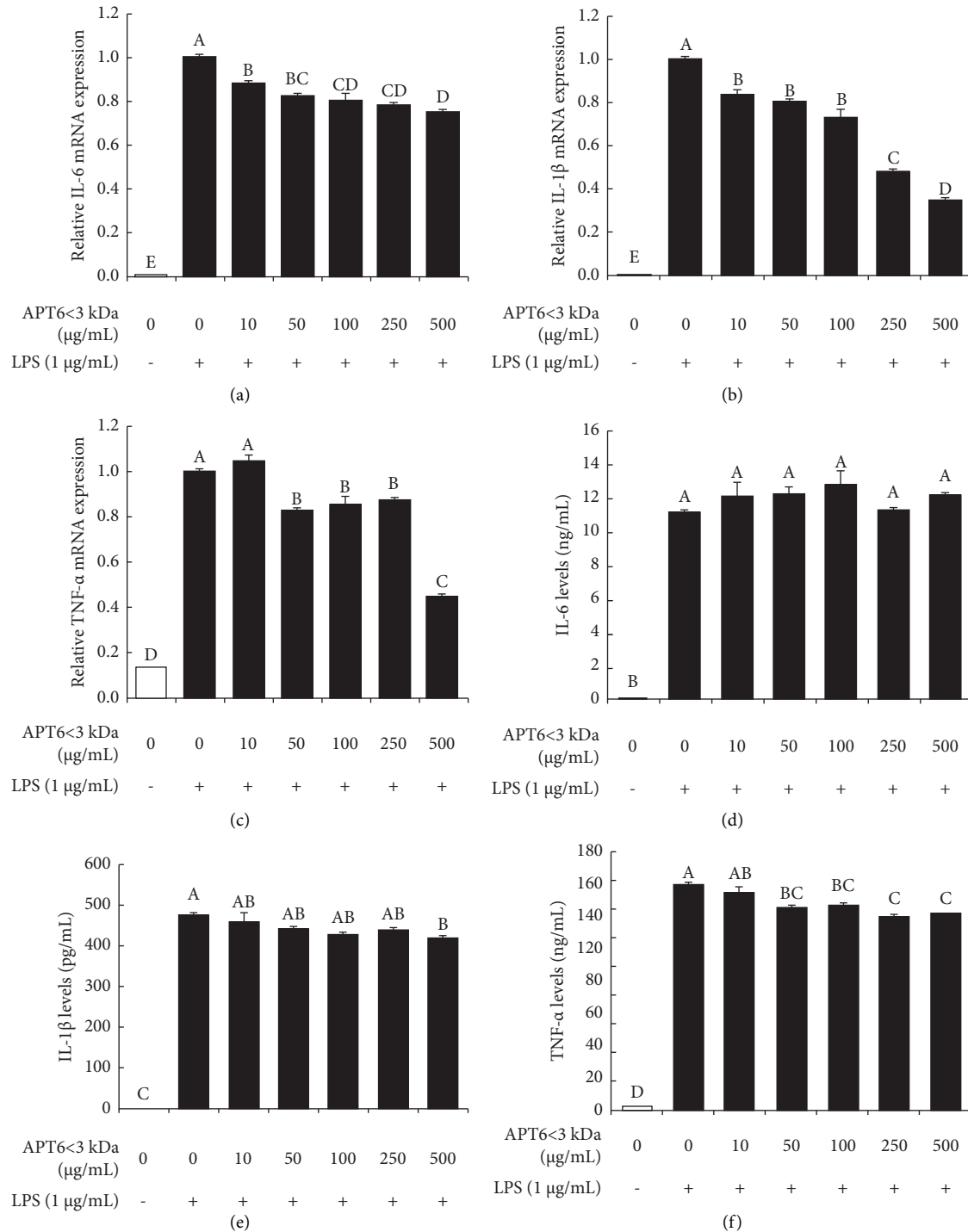


FIGURE 3: Effects of APT6 < 3 kDa on mRNA and levels of proinflammatory cytokines (IL-6, IL-1 $\beta$ , and TNF- $\alpha$ ) in LPS-stimulated RAW 264.7 cells. Cells were treated with APT6 < 3 kDa for 1 h and incubated with LPS (1  $\mu$ g/mL) for 6 h. mRNA levels of IL-6 (a), IL-1 $\beta$  (b), and TNF- $\alpha$  (c) were determined by RT-qPCR. To determine the levels of IL-6 (d), IL-1 $\beta$  (e), and TNF- $\alpha$  (f), cells were treated with APT6 < 3 kDa for 1 h, then incubated with LPS (1  $\mu$ g/mL) for 24 h, and subjected to ELISA. APT6 < 3 kDa is the low-molecular-weight fraction (<3 kDa) of BGE hydrolysate prepared by treatment with Alcalase, ProteAX, and trypsin for 2 h each. <sup>A-E</sup>Different superscript letters above bars indicate a significant difference at  $p < 0.05$ .

$\alpha$  is shown in Figure 3. The mRNA expression of IL-6, IL-1 $\beta$ , and TNF- $\alpha$  significantly increased following LPS treatment of RAW 264.7 cells for 6 h. Treatment with APT6 < 3 kDa at concentrations of 10–500  $\mu$ g/mL decreased the mRNA

expression of IL-6 and IL-1 $\beta$ , and concentrations of 50–500  $\mu$ g/mL of APT6 < 3 kDa reduced TNF- $\alpha$  expression ( $p < 0.05$ ; Figures 3(a)–3(c)). However, IL-6 levels were not suppressed by treatment with APT6 < 3 kDa ( $p > 0.05$ ;



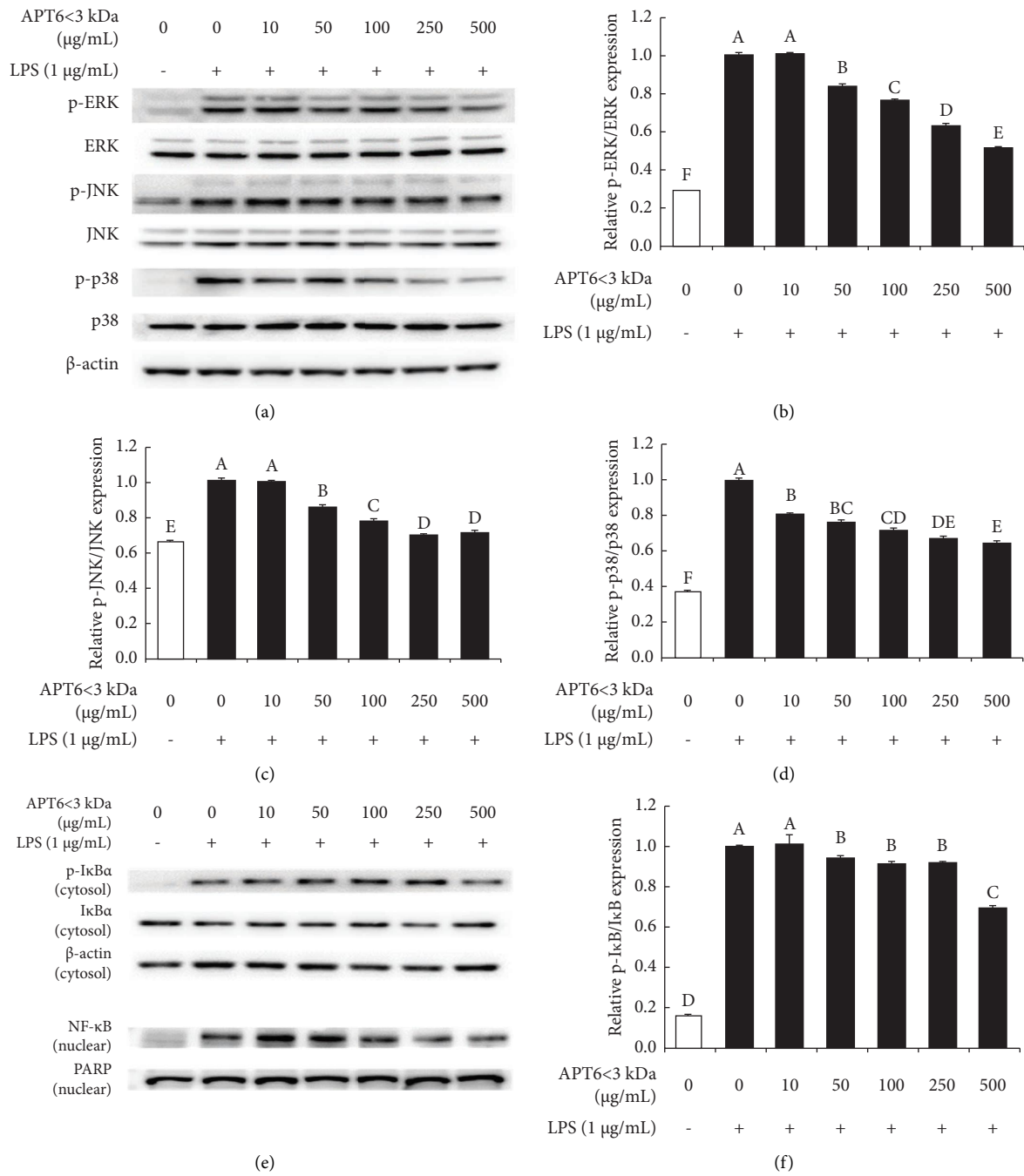


FIGURE 4: Continued.

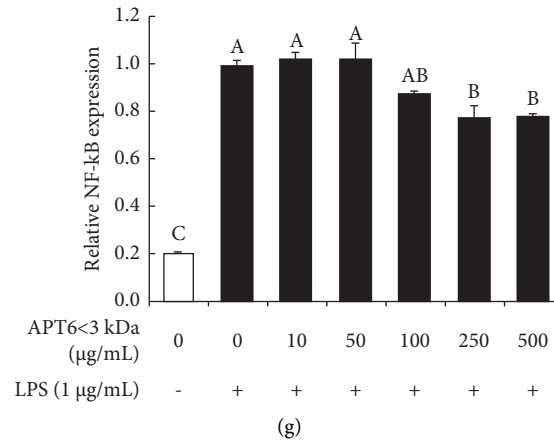


FIGURE 4: Effect of APT6 < 3 kDa on the activation of MAPKs and NF- $\kappa$ B in RAW 264.7 cells after stimulation with LPS (1  $\mu$ g/mL) for 1 h. MAPK protein levels were measured by western blotting (a). Relative levels of MAPKs were determined by densitometry (b–d). I $\kappa$ B and NF- $\kappa$ B protein levels were measured by western blotting (e). Relative amounts of I $\kappa$ B and NF- $\kappa$ B were determined by densitometry (f–g). APT6 < 3 kDa is the low-molecular-weight fraction (<3 kDa) of BGE hydrolysate prepared by treatment with Alcalase, ProteAX, and trypsin for 2 h each. <sup>A–F</sup>Different superscript letters above bars indicate a significant difference at  $p < 0.05$ .

Figure 3(d)). Treatment with 500  $\mu$ g/mL of APT6 < 3 kDa decreased IL-1 $\beta$  levels compared to the LPS-only treatment (414.70 pg/mL vs. 472.79 pg/mL;  $p < 0.05$ ; Figure 3(e)). In addition, treatment with 500  $\mu$ g/mL of APT6 < 3 kDa resulted in a significant suppression of TNF- $\alpha$  levels to 87.33% compared to the LPS-only treatment ( $p < 0.05$ ; Figure 3(f)). These results suggest that the reduction in IL-1 $\beta$  and TNF- $\alpha$  production observed following treatment with APT6 < 3 kDa may be associated with the downregulation of IL-1 $\beta$  and TNF- $\alpha$  transcription. However, the inhibition of IL-6 transcription did not result in a substantial reduction of IL-6 levels in RAW 264.7 cells.

**3.7. Effects of APT6 < 3 kDa on the Phosphorylation of MAPKs and Activation of NF- $\kappa$ B.** LPS is known to bind to the surface receptors such as TLR-4, CD14, and CR3 on macrophages, leading to the activation of MAPKs phosphorylation and subsequent enhancement of iNOS and transcription factor NF- $\kappa$ B activation [27]. As shown in Figures 4(a)–4(d), LPS increased MAPKs phosphorylation by approximately 1.5–3.4-fold compared to CON ( $p < 0.05$ ). However, APT6 < 3 kDa exhibited dose-dependent inhibition of JNK, ERK, and p38 phosphorylation ( $p < 0.05$ ). Especially, treatment with 500  $\mu$ g/mL of APT6 < 3 kDa reduced the phosphorylation of JNK, ERK, and p38 to 70.99%, 51.45%, and 64.81%, respectively, compared to LPS only (100%;  $p < 0.05$ ). The phosphorylation of ERK is associated with cell differentiation and proliferation, while JNK phosphorylation is associated with apoptosis, stress response, and inflammation [28]. In addition, the downregulation of MAPK expression can influence numerous genes associated with inflammation, including those encoding IL-1 $\beta$ , IL-6, TNF- $\alpha$ , COX-2, and iNOS [26]. Therefore, the inhibition of the p38, ERK, and JNK pathways by APT6 < 3 kDa is likely responsible for the reductions in these proinflammatory cytokines and other mediators, highlighting the potential of

APT6 < 3 kDa for therapeutic applications in anti-inflammatory interventions.

In the inflammation condition, cytosolic I $\kappa$ B is phosphorylated, leading to the release of the NF- $\kappa$ B molecule which translocates from the cytosol to the nucleus, where it regulates the transcription of genes encoding IL-6, TNF- $\alpha$ , IL-1 $\beta$ , iNOS, and COX-2 [26]. The phosphorylation of cytosolic I $\kappa$ B increased approximately 6.07-fold upon LPS stimulation (Figures 4(e)–4(f);  $p < 0.05$ ), indicating activation of the NF- $\kappa$ B pathway. Nuclear NF- $\kappa$ B protein showed a 5.06-fold increase after stimulation with 1  $\mu$ g/mL of LPS for 1 h (Figure 4(g);  $p < 0.05$ ). Treatment with 50–500  $\mu$ g/mL of APT6 < 3 kDa inhibited the phosphorylation of cytosolic I $\kappa$ B (Figure 4(f);  $p < 0.05$ ). Furthermore, APT6 < 3 kDa at 250 and 500  $\mu$ g/mL significantly suppressed the expression of nuclear NF- $\kappa$ B protein to 77.61%–77.95% compared to LPS-only treatment (100%; Figure 4(g)). These results indicate that APT6 < 3 kDa regulates the activation of proteins in the MAPK and NF- $\kappa$ B pathways in LPS-stimulated RAW 264.7 cells, suggesting that the effects of APT6 < 3 kDa on NO, PGE<sub>2</sub>, and proinflammatory cytokine and protein expression are mediated through the downregulation of MAPK phosphorylation and NF- $\kappa$ B translocation in stimulated cells.

**3.8. Isolation and Identification of Antioxidative and Anti-Inflammatory Peptides in APT6 < 3 kDa.** The APT6 < 3 kDa was separated into five fractions (F1–F5) by fast protein liquid chromatography using a Superdex peptide 30/100 GL column (Figure 5(a)). The ORAC values of these fractions are presented in Figure 5(b). Among the fractions, F5 showed the highest ORAC activity ( $p < 0.05$ ) of 979.88  $\mu$ mol TE/g dry matter, which was 3.6-fold higher than that of APT6 < 3 kDa. F2 and F5 significantly reduced the production of NO and PGE<sub>2</sub> in LPS-stimulated RAW 264.7 cells compared to APT6 < 3 kDa and LPS-only treatment ( $p < 0.05$ ; Figures 5(c) and 5(d)). These results indicate that

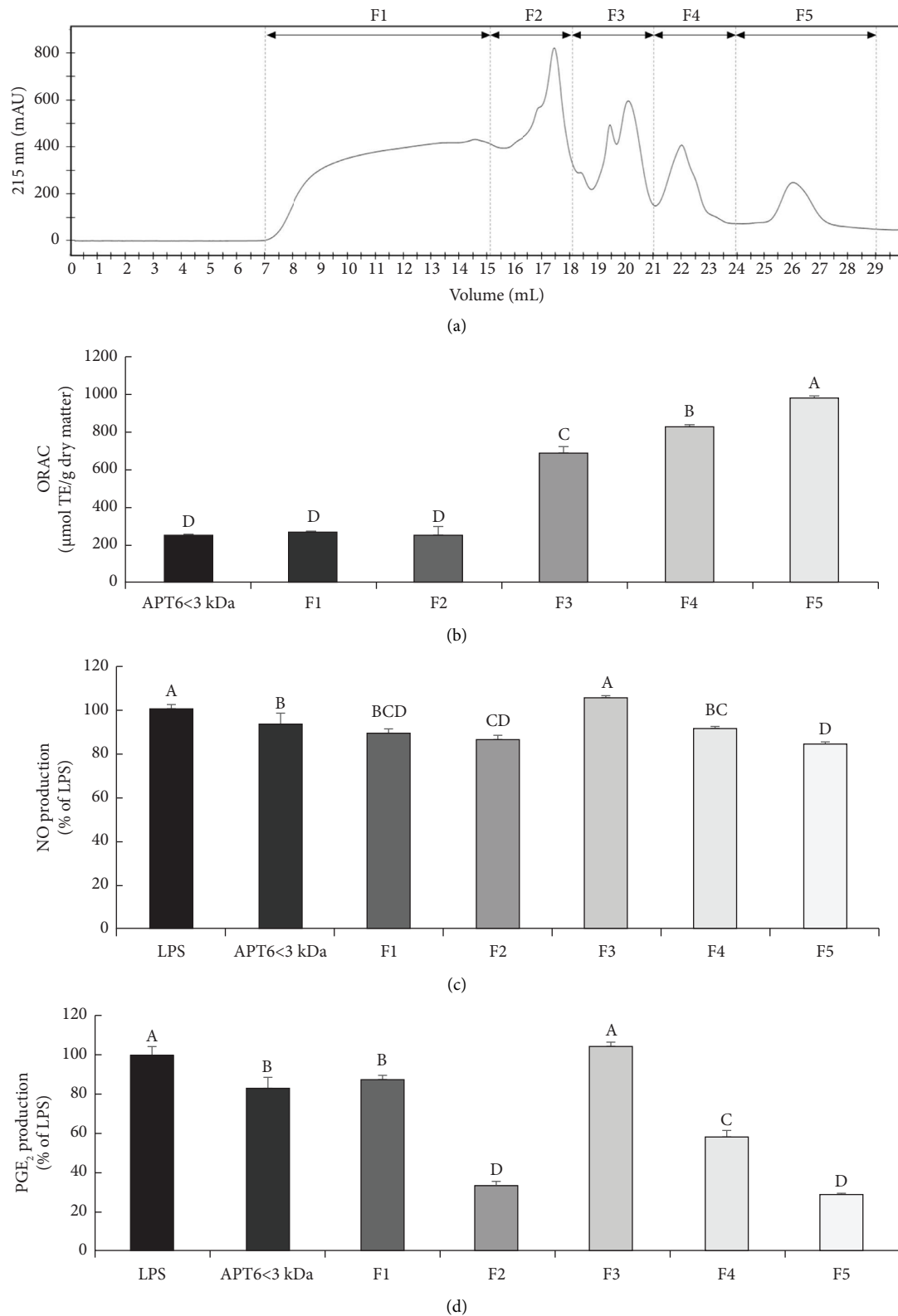


FIGURE 5: Analysis of the antioxidative and anti-inflammatory fractions of APT6 < 3 kDa separated using a superdex peptide 30/100 GL column. Chromatogram of APT6 < 3 kDa showing five fractions (a) and ORAC value of APT6 < 3 kDa and the five fractions (b). To evaluate NO (c) and PGE<sub>2</sub> (d) production, RAW 264.7 cells were treated with APT6 < 3 kDa and the five fractions (250  $\mu\text{g/mL}$ ) for 1 h and then stimulated with LPS (1  $\mu\text{g/mL}$ ) for 24 h. <sup>A-D</sup>Different superscript letters above bars indicate a significant difference at  $p < 0.05$ .

TABLE 2: Amino acid sequences of peptides in F5 and their HAA composition (%).

No.	Sequence	MW (Da)	Probability (%)	HAA (%)
1	GVXGPXGAVGPA	1006.51	99.00	83.33
2	GRPGEVGGPPGPPGAGE	1574.73	99.00	82.35
3	VGPPGPSGNAGPXGPXGPA	1643.74	99.00	78.95
4	GAPGADGPAGAXGTPGPQ	1489.68	99.00	77.78
5	GPXGAXGAXGAXGPVGP	1486.71	99.00	77.78
6	GVQGPXGPAGPR	1104.57	99.00	75.00
7	VGPXGPXGPAGE	1062.50	99.00	75.00
8	KGAPGADGPAGAXGTPGPQ	1617.77	99.00	73.68
9	GFAGPXGADGQPAGAK	1341.63	99.00	73.33
10	GPXGPAGPAGERGEQGPA	1616.75	99.00	72.22
11	GPXGPSGNAGPXGPXGPA	1528.68	99.00	72.22
12	GPXGPXGPXGPXGPPSGG	1538.70	99.00	72.22
13	GPSGPQGSPSPXGP	1203.55	99.00	71.43
14	VGPXGPSGNAGPXGPXGPAGK	1812.86	99.00	71.43
15	GIQGPXGPAGEEG	1180.54	99.00	69.23
16	GRXGEVGPXGPXGPAG	1445.69	99.00	68.75
17	GAPGDKGETGPSGPAGPTGAR	1851.87	99.00	66.67
18	GPSGPQGSPSPXGP	1331.65	99.00	66.67
19	GFXGSDGVAGPK	1103.52	99.00	66.67
20	GIQGPXGPAGEE	1123.51	99.00	66.67
21	GVXGDLGAXGPS	1054.49	99.00	66.67
22	QGLXGPAGPXGE	1107.52	99.00	66.67
23	GRXGEVGPXGPXGPA	1388.67	99.00	66.67
24	GLXGPXGAXGPQ	1091.52	99.00	66.67
25	GIQGPXGPAGEEGK	1308.63	99.00	64.29
26	GPXGLAGPXGESGR	1279.62	99.00	64.29
27	TGPXGPAGQDGRXGPXGPXGAR	2055.97	99.00	61.90
28	GAXGDKGETGPSGPAGPT	1567.71	99.00	61.11
29	XGDKGETGPSGPAGPTGA	1549.70	99.00	61.11
30	GSEGPQGVVRGEXGPXGPA	1677.76	99.00	61.11
31	GRXGEVGPXGPXGPAGEK	1702.83	99.00	61.11
32	GIQGPXGPAGEEGKR	1464.73	99.00	60.00
33	GAXGDRGEXGPXGPA	1378.61	99.00	60.00
34	AGKXGEQGVXGDLGAXGPS	1737.82	99.00	57.89
35	QGPXGEXGEXGASGPMGPR	1821.80	99.00	57.89
36	QGPXGPXGSXGEQGPSGASGPAGPR	2243.02	99.00	57.14
37	QGPXGEXGEXGASGPM	1494.59	99.00	56.25
38	GEXGSXGENGAPGQMGR	1742.72	99.00	55.56
39	GSXGEAGRGEAGLXGAK	1654.79	99.00	55.56
40	QGPXGPXGSXGEQGPSGA	1620.70	99.00	55.56
41	SGLQGPXGPXGSXGEQGPS	1749.78	99.00	52.63
42	QGPXGPXGSXGEQGPS	1475.62	99.00	50.00
43	GAPGFPGAR	860.42	97.93	50.00

MW, observed molecular weight; HAA, hydrophobic amino acids; X, hydroxyproline. Hydrophobic amino acids (%) is the percentage of hydrophobic residues (G, V, L, I, P, F, M) in the peptide sequence.

F5 exhibited both the highest antioxidative and anti-inflammatory effects among the five fractions, and therefore, it was selected for further analysis of its constituent peptides. In total, 43 peptides were identified in F5, and the sequences of representative peptides are listed in Table 2. Notably, glycine (G), proline (P), hydroxyproline (X), and alanine (A) were the predominant amino acids in F5. Especially, G-P-X and G-P sequences were frequently detected. The antioxidative and immunomodulatory properties of peptides can be influenced by their structure, amino acid composition, length, and hydrophobicity [7]. For instance, collagen contains a G-P1-P2 triplet sequence, where P1 is predominantly proline (20–30%) and P2 is typically hydroxyproline [29]. The exposure of the glycine residue is

essential for Fe (II)-binding activity [30]. The G-P-X sequence, found in peptides derived from marine sources or animal skin, is known to exhibit high antioxidative activity [31]. According to Jin et al. [32], G-P displays potent dipeptidyl peptidase IV-inhibitory activity, suggesting its potential application in pharmacological agents for inflammatory diseases. In addition, HAA contributes to the antioxidative and anti-inflammatory properties of peptides [7]. In the case of the 43 peptides identified in F5, they exhibited HAA content ranging from 50.00 to 83.33%. These results suggest that the high antioxidative and anti-inflammatory effects observed in F5 and APT6 < 3 kDa may be attributed to the amino acid composition and characteristics of these peptides. However, further

investigations are required to explore the specific anti-oxidative and anti-inflammatory activities of each peptide within F5.

#### 4. Conclusions

The present study provides evidence for the antioxidative and anti-inflammatory properties of APT6 < 3 kDa, a low-molecular-weight hydrolysate of BGE. APT6 < 3 kDa exhibited potent antioxidative activity, reducing oxidative stress in LPS-stimulated RAW 264.7 cells. Moreover, it demonstrated anti-inflammatory effects by inhibiting the NF- $\kappa$ B and MAPK pathways, resulting in a decrease in the production of proinflammatory cytokines and down-regulation of inflammatory protein expression. Notably, a specific fraction of APT6 < 3 kDa (F5), which contained 43 short peptides, showed high antioxidative and anti-inflammatory activities, likely attributed to its high proportion of HAA. These findings highlight the potential application of APT6 < 3 kDa and its peptides in the functional food industry. Furthermore, from a broader perspective in the future, it will be worthwhile to explore the immune regulatory effects of APT6 < 3 kDa. However, future investigations will be warranted to evaluate the anti-inflammatory effects and absorption profile of APT6 < 3 kDa and its purified peptides in other cell lines and animal models.

#### Data Availability

The data supporting the results of this study can be obtained from the corresponding authors upon reasonable request.

#### Conflicts of Interest

The authors have no conflicts of interest to disclose.

#### Authors' Contributions

Kim H.J. was in charge of writing the original draft, data curation, formal analysis, visualization, and reviewing and editing. Kim K.W. and Lee J. were in charge of investigation, reviewing, and editing. Lee S.H. and Lee S.S. edited the manuscript and supervised the study. Jang A. handled resources and reviewed, edited, and supervised the study.

#### Acknowledgments

This work was supported by the National Research Foundation of Korea (NRF) grant funded by the Korea Government (MEST) (NRF-2018R1A2B6008077).

#### Supplementary Materials

Table S1: sequences of primers used for RT-qPCR. Table S2: amino acid composition (g/100 g sample) of APT6 and APT6 < 3 kDa from BGE. Figure S1: schematic diagram of the preparation of low-molecular-weight hydrolysates and the identification of antioxidant and anti-inflammatory peptides from BGE. (*Supplementary Materials*)

#### References

- [1] S. O. Abarikwu, "Kolaviron, a natural flavonoid from the seeds of *Garcinia kola*, reduces LPS-induced inflammation in macrophages by combined inhibition of IL-6 secretion, and inflammatory transcription factors, ERK1/2, NF- $\kappa$ B, p38, Akt, p-c-JUN and JNK," *Biochimica et Biophysica Acta (BBA)-General Subjects*, vol. 1840, no. 7, pp. 2373–2381, 2014.
- [2] Y. S. Kim, C. B. Ahn, and J. Y. Je, "Anti-inflammatory action of high molecular weight *Mytilus edulis* hydrolysates fraction in LPS-induced RAW 264.7 macrophage via NF- $\kappa$ B and MAPK pathways," *Food Chemistry*, vol. 202, pp. 9–14, 2016.
- [3] S. Y. Park, C. B. Ahn, and J. Y. Je, "Antioxidant and anti-inflammatory activities of protein hydrolysates from *Mytilus edulis* and ultrafiltration membrane fractions," *Journal of Food Biochemistry*, vol. 38, no. 5, pp. 460–468, 2014.
- [4] K. Sheeja, P. K. Shihab, and G. Kuttan, "Antioxidant and anti-inflammatory activities of the plant *Andrographis paniculata* nees," *Immunopharmacology and Immunotoxicology*, vol. 28, no. 1, pp. 129–140, 2006.
- [5] M. S. Arshad, W. Khalid, R. S. Ahmad et al., "Functional foods and human health: an overview," *Functional Foods Phytochem Health Promoting Potential*, vol. 3, 2021.
- [6] N. Y. Sung, P. M. Jung, M. Yoon et al., "Anti-inflammatory effect of sweetfish-derived protein and its enzymatic hydrolysate on LPS-induced RAW 264.7 cells via inhibition of NF- $\kappa$ B transcription," *Fisheries Science*, vol. 78, no. 2, pp. 381–390, 2012.
- [7] M. Chalamaiah, W. Yu, and J. Wu, "Immunomodulatory and anticancer protein hydrolysates (peptides) from food proteins: a review," *Food Chemistry*, vol. 245, pp. 205–222, 2018.
- [8] S. H. Kim, I. W. Hwang, S. K. Chung et al., "Physicochemical properties of *Salvia miltiorrhiza* Bunge following treatment with enzymes," *Korean Journal of Food Preservation*, vol. 22, no. 5, pp. 699–707, 2015.
- [9] J. S. Kim, D. Kim, H. J. Kim, and A. Jang, "Protection effect of donkey hide gelatin hydrolysates on UVB-induced photoaging of human skin fibroblasts," *Process Biochemistry*, vol. 67, pp. 118–126, 2018.
- [10] D. Kim, Y. H. B. Kim, J. S. Ham, S. K. Lee, and A. Jang, "Pig skin gelatin hydrolysates attenuate acetylcholine esterase activity and scopolamine-induced impairment of memory and learning ability of mice," *Food Science of Animal Resources*, vol. 40, no. 2, pp. 183–196, 2020.
- [11] T. S. Vo, B. Ryu, and S. K. Kim, "Purification of novel anti-inflammatory peptides from enzymatic hydrolysate of the edible microalgal *Spirulina maxima*," *Journal of Functional Foods*, vol. 5, no. 3, pp. 1336–1346, 2013.
- [12] H. J. Kim, S. R. Yang, and A. Jang, "Anti-proliferative effect of a novel anti-oxidative peptide in Hanwoo beef on human colorectal carcinoma cells," *Korean Journal for Food Science of Animal Resources*, vol. 38, no. 6, pp. 1168–1178, 2018.
- [13] H. J. Kim, H. J. Kim, and A. Jang, "Nutritional and antioxidative properties of black goat meat cuts," *Asian-Australasian Journal of Animal Sciences*, vol. 32, no. 9, pp. 1423–1429, 2019.
- [14] Y. B. Kim, I. J. Yoo, K. H. Jeon, and B. H. Lee, "Nutritional value of Korean native black goat meat and meat-bone extract," *Korean Journal for Food Science of Animal Resources*, vol. 15, pp. 132–138, 1995.
- [15] H. J. Kim, H. J. Kim, K. W. Kim et al., "Effect of feeding alfalfa and concentrate on meat quality and bioactive compounds in Korean native black goat loin during storage at 4°C," *Food Science of Animal Resources*, vol. 42, no. 3, pp. 517–535, 2022.

- [16] Y. R. Li, C. S. Fu, W. J. Yang et al., "Investigation of constituents from *Cinnamomum camphora* (L.) J. Presl and evaluation of their anti-inflammatory properties in lipopolysaccharide-stimulated RAW 264.7 macrophages," *Journal of Ethnopharmacology*, vol. 221, pp. 37–47, 2018.
- [17] K. S. Jo, "A study on the extraction time and component analysis of goat meat with bone extract," *Korean Journal of Food Preservation*, vol. 9, pp. 396–399, 2002.
- [18] M. Linder, P. Rozan, R. L. El Kossori et al., "Nutritional value of veal bone hydrolysate," *Journal of Food Science*, vol. 62, no. 1, pp. 183–189, 1997.
- [19] D. M. Rossi, S. H. Flôres, J. G. Venzke, and M. A. Z. Ayub, "Biological evaluation of mechanically deboned chicken meat protein hydrolysate," *Nutrition Magazine*, vol. 22, no. 6, pp. 879–885, 2009.
- [20] A. E. Theodore, S. Raghavan, and H. G. Kristinsson, "Antioxidative activity of protein hydrolysates prepared from alkaline-aided channel catfish protein isolates," *Journal of Agricultural and Food Chemistry*, vol. 56, no. 16, pp. 7459–7466, 2008.
- [21] X. P. Dong, B. W. Zhu, H. X. Zhao et al., "Preparation and in vitro antioxidant activity of enzymatic hydrolysates from oyster (*Crassostrea talienwhannensis*) meat," *International Journal of Food Science and Technology*, vol. 45, no. 5, pp. 978–984, 2010.
- [22] R. He, A. T. Girgih, S. A. Malomo, X. Ju, and R. E. Aluko, "Antioxidant activities of enzymatic rapeseed protein hydrolysates and the membrane ultrafiltration fractions," *Journal of Functional Foods*, vol. 5, no. 1, pp. 219–227, 2013.
- [23] D. W. Kim, K. Park, G. Ha et al., "Anti-oxidative and neuroprotective activities of pig skin gelatin hydrolysates," *Korean Journal for Food Science of Animal Resources*, vol. 33, no. 2, pp. 258–267, 2013.
- [24] X. Y. Mao, X. Cheng, X. Wang, and S. J. Wu, "Free-radical-scavenging and anti-inflammatory effect of yak milk casein before and after enzymatic hydrolysis," *Food Chemistry*, vol. 126, no. 2, pp. 484–490, 2011.
- [25] J. H. Hwang, J. N. Ma, J. H. Park, H. W. Jung, and Y. K. Park, "Anti-inflammatory and antioxidant effects of MOK, a polyherbal extract, on lipopolysaccharide stimulated RAW 264.7 macrophages," *International Journal of Molecular Medicine*, vol. 43, no. 1, pp. 26–36, 2019.
- [26] P. Wan, M. Xie, G. Chen et al., "Anti-inflammatory effects of dicaffeoylquinic acids from *Ilex kudingcha* on lipopolysaccharide-treated RAW264.7 macrophages and potential mechanisms," *Food and Chemical Toxicology*, vol. 126, pp. 332–342, 2019.
- [27] S. H. Chang, Y. Y. Lin, G. J. Wu, C. H. Huang, and G. J. Tsai, "Effect of chitosan molecular weight on anti-inflammatory activity in the RAW 264.7 macrophage model," *International Journal of Biological Macromolecules*, vol. 131, pp. 167–175, 2019.
- [28] E. Herlaar and Z. Brown, "p38 MAPK signalling cascades in inflammatory disease," *Molecular Medicine Today*, vol. 5, no. 10, pp. 439–447, 1999.
- [29] L. Guo, P. A. Harnedy, M. B. O'Keefe et al., "Fractionation and identification of Alaska pollock skin collagen-derived mineral chelating peptides," *Food Chemistry*, vol. 173, pp. 536–542, 2015.
- [30] C. Y. Huang, C. H. Wu, J. I. Yang, Y. H. Li, and J. M. Kuo, "Evaluation of iron-binding activity of collagen peptides prepared from the scales of four cultivated fishes in Taiwan," *Journal of Food and Drug Analysis*, vol. 23, no. 4, pp. 671–678, 2015.
- [31] B. Li, F. Chen, X. Wang, B. Ji, and Y. Wu, "Isolation and identification of antioxidative peptides from porcine collagen hydrolysate by consecutive chromatography and electrospray ionization–mass spectrometry," *Food Chemistry*, vol. 102, no. 4, pp. 1135–1143, 2007.
- [32] Y. Jin, J. Yan, Y. Yu, and Y. Qi, "Screening and identification of DPP-IV inhibitory peptides from deer skin hydrolysates by an integrated approach of LC–MS/MS and in silico analysis," *Journal of Functional Foods*, vol. 18, pp. 344–357, 2015.